

# CrystEngComm

Accepted Manuscript



This is an *Accepted Manuscript*, which has been through the Royal Society of Chemistry peer review process and has been accepted for publication.

*Accepted Manuscripts* are published online shortly after acceptance, before technical editing, formatting and proof reading. Using this free service, authors can make their results available to the community, in citable form, before we publish the edited article. We will replace this *Accepted Manuscript* with the edited and formatted *Advance Article* as soon as it is available.

You can find more information about *Accepted Manuscripts* in the [Information for Authors](#).

Please note that technical editing may introduce minor changes to the text and/or graphics, which may alter content. The journal's standard [Terms & Conditions](#) and the [Ethical guidelines](#) still apply. In no event shall the Royal Society of Chemistry be held responsible for any errors or omissions in this *Accepted Manuscript* or any consequences arising from the use of any information it contains.



Journal Name

ARTICLE

## The influence of the reaction media on CdIn<sub>2</sub>S<sub>4</sub> and ZnIn<sub>2</sub>S<sub>4</sub> nanocrystalite formation and growth of mesocrystal structures

M. V. Carević,<sup>a</sup> M. I. Čomor,<sup>a\*</sup> M. N. Mitrić,<sup>a</sup> T. S. Barudžija,<sup>a</sup> S. P. Ahrenkiel,<sup>b</sup> and Nadica D. Abazović<sup>a\*</sup>

Received 00th January 20xx,  
Accepted 00th January 20xx

DOI: 10.1039/x0xx00000x

www.rsc.org/

Hot-injection method for synthesis of CdIn<sub>2</sub>S<sub>4</sub> in three different compositions of organic media/solvents was studied. Nanosized CdIn<sub>2</sub>S<sub>4</sub> is successfully synthesized in oleic acid/oleylamine mixture of complexing/capping agents. Obtained mesocrystals of 20-30 nm in diameter are self-organized in marigold-like structures. Estimated band-gap of synthesized semiconductor is far in visible spectral region and has a value of 2.1 eV. Potential of band edges is calculated using empirical equation. As-prepared material was successfully transferred from organic to aqueous media by using 2-mercaptoethanol in surface ligand exchange process. Using similar synthetic procedure, ZnIn<sub>2</sub>S<sub>4</sub> synthesis was performed. Obtained materials are characterized using UV/Vis spectroscopy, XRD and TEM. Formation and growth mechanism of synthesized materials are proposed.

### Introduction

It is well known that binary II-VI metal sulfides (CdS, ZnS) are unstable during photocatalytic processes and easily undergo photocorrosion under influence of photogenerated holes. Efforts have been made in order to stabilize these materials, mostly by incorporation of metal sulfides into interlayer, but even if this step stabilizes photocatalyst, its photocatalytic efficiency was reduced.<sup>1</sup> As a replacement, ternary metal sulfides can be considered since they have narrow band gaps and strong absorption in visible spectral region.<sup>2</sup> Beside their possible application as photocatalysts in degradation processes of various pollutants, these properties recommend this class of materials for application in photoproduction of H<sub>2</sub> from water and H<sub>2</sub>S. Two semiconductors from this II-III<sub>2</sub>-VI<sub>4</sub> family that are especially interesting is CdIn<sub>2</sub>S<sub>4</sub> (CIS) and ZnIn<sub>2</sub>S<sub>4</sub> (ZIS). CIS has direct band gap of 2.1-2.2 eV (about 560 nm) meaning that it has strong absorption in visible part of the spectra. It usually crystallizes in cubic spinel structure which belongs to the *Fd3m* space group. In contrast, bulk ZIS has an indirect band-gap, with reported energy values from 2.1 to 1.8 eV (590 to 690 nm) which makes it very suitable material for solar energy conversion applications. It has three polymorphs: rhombohedral, cubic and hexagonal, wherein the hexagonal

form (space group *P63mc*) is the most common one.

Both materials are typically synthesized via solvothermal/hydrothermal route<sup>2-8</sup> but a few groups have used different approaches: hot-wall epitaxy method<sup>9</sup>, microwave-solvothermal approach<sup>10,11</sup> and ultrasonic spray pyrolysis (USP)<sup>12</sup>. Interestingly, there is a very few articles<sup>13-16</sup> where hot-injection approach is used for synthesis of these materials. Hot-injection method is widely used in synthesis of II-VI semiconductors since first article of Murray *et al.*<sup>17</sup> where authors presented a new way to synthesize highly crystalline CdE (E=S,Se,Te) nanoparticles. In the huge number of articles that followed and that deal with the hot-injection method, it has been shown that this route of synthesis provides not just control over sizes and shapes, but also over crystallinity and crystal phase of obtained particles. The only "catch" is to choose the appropriate combination of ion precursors and surfactants/organic solvents, since temperature/time frame is not the only factor that can influence the reaction rate and sizes of obtained nanoparticles. This approach was our method of choice for synthesis of CIS and ZIS as a continuation of our previously published results.<sup>18,19</sup>

In the present paper, we have studied the influence of different organic reaction media on crystallinity and crystal phase of obtained materials. The importance of this dependence, as Bhirud *et al.*<sup>5</sup> proposed, is crucial for application of these materials. Photocatalytic activity of CIS particles highly depends on photocatalyst's crystallinity rather than on particle size or surface area, since a lack of defect sites promotes separation and migration of photogenerated carriers toward surface. We shall try to show that by proper combination of organic surfactants it is possible to obtain highly crystalline samples. For most applications, water media is required, so here we also proposed an easy way to transfer

<sup>a</sup> Vinča Institute of Nuclear Sciences, University of Belgrade, P.O. Box 522, Belgrade, Serbia, [mirianac@vinca.rs](mailto:mirianac@vinca.rs); [kiki@vinca.rs](mailto:kiki@vinca.rs)

<sup>b</sup> South Dakota School of Mines and Technology, 501 E. Saint Joseph Street, Rapid City, SD 57701, USA

Electronic Supplementary Information (ESI) available: Table S1. Molarities of precursor solutions; XRD patterns of synthesized samples together with corresponding JCPDS cards and relative intensities of related diffraction peaks; Tauc plots of samples C2; Additional TEM images of sample C3 (CdIn<sub>2</sub>S<sub>4</sub>) before and after surface ligand exchange. See DOI: 10.1039/x0xx00000x

obtained samples from organic media to water, by using 2-mercaptoethanol as capping agent.

## Experimental

### Materials

All chemicals were of analytical grade (highest available) and were used without further purification. All precursor solutions were prepared fresh before synthesis.

Cadmium acetate dihydrate ( $\text{Cd}(\text{Ac})_2$ ), zinc acetate ( $\text{Zn}(\text{Ac})_2$ ), indium-acetate ( $\text{In}(\text{Ac})_3$ ), oleic acid ( $\text{OA}-\text{C}_{17}\text{H}_{33}\text{COOH}$ ), 1-octadecene ( $\text{ODE}-\text{C}_{18}\text{H}_{36}$ ), oleylamine ( $\text{OLAM}-\text{C}_{18}\text{H}_{35}\text{NH}_2$ ) and 2-mercaptoethanol ( $2\text{ME}-\text{HS}-\text{C}_2\text{H}_4-\text{OH}$ ) were purchased from Sigma -Aldrich. Sulfur powder was obtained from Alfa Aesar. Toluene and acetone were purchased from JT Baker.

### Sample C1:

*Cadmium - Cd1:*  $\text{Cd}(\text{Ac})_2$  (0.1mmol; 0.0266g), OA (0.2 mmol; 0.0632ml) and ODE (2ml) were loaded in three-neck flask and heated at 200°C under constant Ar flow. After about 30 min, brown solution is formed, and was left at room temperature to cool down.

*Indium-In1:*  $\text{In}(\text{Ac})_3$  (0.2 mmol; 0.0584 g), OA (0.6 mmol; 0.189 ml) and ODE (2ml) were loaded in three-neck flask and heated at 270°C under constant Ar flow. After about 30 min, pale yellow solution is formed.

*Sulfur-S1:* Sulfur powder (0.4mmol; 0.0128g) and ODE (2ml) were loaded in three-neck flask and heated at 90°C under constant Ar flow. After about 30 min solution was left at room temperature to cool down.

### Sample C2:

*Cadmium- Cd2:*  $\text{Cd}(\text{Ac})_2$  (0.0667mmol; 0.0177g) and OA (2ml) were loaded in three-neck flask and heated at 200°C under constant Ar flow. After about 30 min, brown solution is formed, and was left at room temperature to cool down.

*Indium-In2:*  $\text{In}(\text{Ac})_3$  (0.2 mmol; 0.0584 g) and OA (2ml) were loaded in three-neck flask and heated at 270°C under constant Ar flow. After about 30 min, pale yellow solution is formed.

*Sulfur-S2:* Sulfur powder (0.4mmol; 0.0128g) and OA (2ml) were loaded in three-neck flask and heated at 90°C under constant Ar flow. After about 30 min solution was left at room temperature to cool down.

### Sample C3:

*Cadmium-Cd2:*  $\text{Cd}(\text{Ac})_2$  (0.0667mmol; 0.0177g) and OA (2ml) were loaded in three-neck flask and heated at 200°C under constant Ar flow. After about 30 min, brown solution is formed, and was left at room temperature to cool down.

*Indium-In2:*  $\text{In}(\text{Ac})_3$  (0.2 mmol; 0.0584 g) and OA (2ml) were loaded in three-neck flask and heated at 270°C under constant Ar flow. After about 30 min, pale yellow solution is formed.

*Sulfur-S3:* Sulfur powder (0.4mmol; 0.0128g) and OLAM (1ml) were loaded in three-neck flask and heated at 90°C under constant Ar flow. After about 30 min solution was left at room temperature to cool down.

### Sample Z1:

*Zinc - Zn1:*  $\text{Zn}(\text{Ac})_2$  (0.1mmol; 0.0219g) and OA (2ml) were loaded in three-neck flask and heated at 200°C under constant Ar flow. After about 30 min, obtained solution was left at room temperature to cool down.

*Indium-In2:*  $\text{In}(\text{Ac})_3$  (0.2 mmol; 0.0584 g) and OA (2ml) were loaded in three-neck flask and heated at 270°C under constant Ar flow. After about 30 min, pale yellow solution is formed.

*Sulfur - S4:* Sulfur powder (0.4mmol, 0.0128g) and OLAM (2 ml) of were loaded in three-neck flask and heated at 90°C under constant Ar flow. After about 30 min solution was left at room temperature to cool down.

(Molarities of all precursor solutions are given in Table S1 in ESI.)

### General procedure for synthesis

In a typical synthesis separate precursor solutions of Cd/Zn, In, and S were prepared in a convenient organic solvent, under constant Ar flow. Then, at 270°C in In solution, Cd and S solutions were swiftly injected, and reaction mixture was kept at that temperature for a fixed time. Exact combination of precursors and reaction times are presented in **Table 1**. After synthesis, mixtures were left to cool down to room temperature, and then obtained precipitates were washed three times with toluene/acetone mixture (3/1, v/v) in order to discard excess of organic molecules. Finally, obtained nanocrystals were re-dispersed in toluene (for TEM and optical measurements) or dried at 60° for XRD measurements.

**Table 1** Assigning of samples according to precursor combination and reaction time

Sample	Precursor combination	Reaction time
C1	Cd1+In1+S1	4h
C2	Cd2+In2+S2	4h
C3	Cd2+In2+S3	1h
Z1	Zn1+In2+S4	30 min

### Organics to water transfer of C3:

4 ml of CIS/toluene dispersion was dried under Ar flow. Then, 4ml of 1M aqueous solution of 2-mercaptoethanol (pH = 8-9) was added to this dried sample. After slight shaking, nanoparticles were dispersed in water and used for optical and

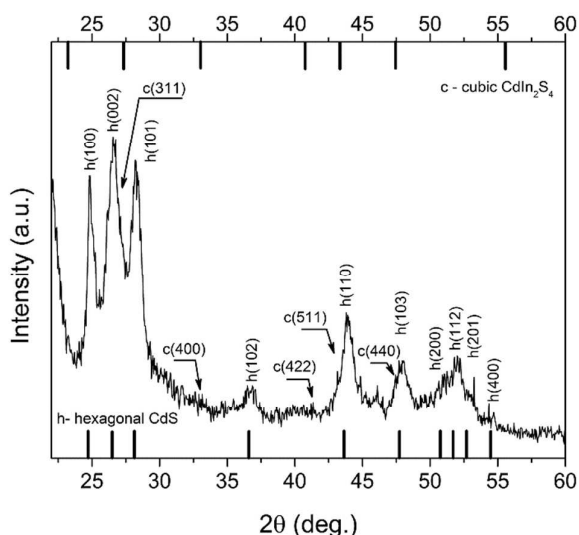


**Fig. 1** XRD pattern of sample C1, synthesized in 1-octadecene

TEM measurements. This dispersion was stable for months (no precipitation or degradation).

**XRD:** XRD patterns were recorded using Philips PW 1050 powder diffractometer with Ni filtered  $\text{CuK}\alpha$  radiation ( $\lambda=1.5418 \text{ \AA}$ ) and scintillation detector. Diffraction data were collected with step of  $0.05^\circ$  and 6 s counting time per step.

**TEM:** TEM (JEOL JEM-2100 LaB6) samples were prepared by dipping a carbon-coated copper grid into toluene or water dispersions and the grids with the nanocrystals were dried in air. The acceleration voltage used was 200kV.

**Optical measurements:** UV-Vis absorption spectra were obtained using Evolution 600 UV/Vis spectrophotometer (Thermo Scientific). Samples were prepared by simple re-dispersing of obtained materials in toluene or water.

## Results and discussion

### $\text{CdIn}_2\text{S}_4$

Typically, in hot-injection synthesis of II-VI semiconductors TOP/TOPO combination of solvent/capping agent is used. Both molecules contain phosphorus ion, and, because of this fact, their usage and later discard could be considered as extremely harmful to the environment. As method is developed through the years, hydrocarbon molecules with some other functional groups (amino, carboxyl, etc.) are used instead, in order to control reaction course and growth of the particles, as these molecules are regarded as less threat to human surroundings. Lately, all these considerations went one step further, and utilization of 1-octadecene or paraffin (both are hydrocarbon chains without any functional groups) as solvent/reaction media, meaning majority of the organic phase, took place. Such a method is firstly introduced by Yu et al.<sup>20</sup>, for synthesis of CdS.

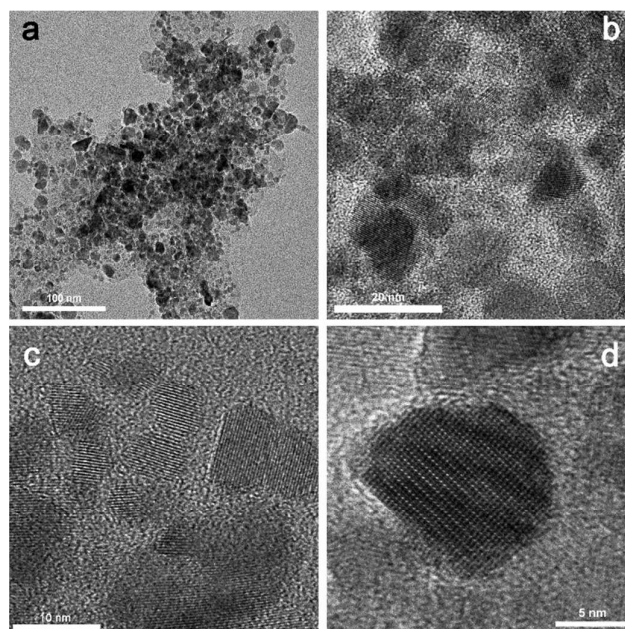


**Fig. 2** TEM images of sample C1, synthesized in presence of 1-octadecene

Guided by this “greener” approach, we also have tried to synthesize CIS in conditions where oleic acid is used only in stoichiometric amounts, i.e. only as complexing agent for cations, while ODE was used both as solvent for elemental sulfur and overall reaction media. X-ray diffractogram of sample (C1) synthesized in this way is presented in Fig. 1 (and Fig S1 in ESI). However, as can be seen in Fig. 1, all major diffraction peaks originated from hexagonal CdS (JCPDS card No. 75-1545). However, more careful consideration of diffraction pattern reveals presence of cubic  $\text{CdIn}_2\text{S}_4$  (JCPDS card No. 27-0060). Namely, low-intensity peaks might be seen at about  $33^\circ$  and  $40.7^\circ$  that originate from reflections (400) and (422) of cubic  $\text{CdIn}_2\text{S}_4$  phase. Additionally, diffraction peaks about  $27^\circ$ ,  $44^\circ$  and  $48^\circ$  are obviously broader due to overlapping of (002), (110) and (103) reflections of major hexagonal CdS phase and (311), (511) and (440) reflections of cubic  $\text{CdIn}_2\text{S}_4$  phase, respectively.

Evidently, these reaction conditions did not favour formation of CIS, even if temperature was high enough ( $270^\circ\text{C}$ ) for degradation of cation-acid complexes, and reaction time of 4h should be enough for completion of the reaction between ions. Clearly, temperature/time frame is not a major factor in determining the course and output of reaction. Rather, in this case, it is the chemical properties of oleic acid and ODE, oleic acid dual role as both complexing and capping agent, but more than anything ratio between In ions and oleic acid. Namely, Battaglia and Peng<sup>21</sup> have investigated the influence that different fatty acids have on formation of InP. They found that not just length of hydrocarbon chain, but also relative molar ratio between In and fatty acid determines whether InP will be formed or not. For example, if molar ratio between In and myristic acid in reaction mixture was 1:2, there were no

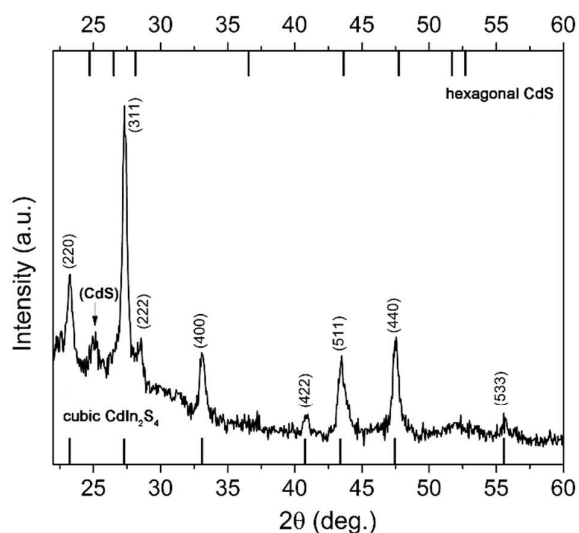


**Fig. 3** XRD pattern of sample C2, synthesized in oleic acid

distinguishable absorption peak of InP nanoparticles as a proof of their formation. Also, if this ratio is 1:4.5 at longer reaction times, absorption peak is not well defined. Authors have concluded that for each examined acid there is certain molar ratio between In and fatty acid for which it is possible to synthesize InP nanoparticles of high quality. Such ratio surely exists also for In and oleic acid, and we presumed that we did not get in that specific concentration window, so reactivity of In ions necessary for formation of CIS is not reached. However, this question needs detailed study, especially because here we are trying to synthesize ternary (not binary) sulfides. Additional drawback of this combination of solvent/complexion agent is that neither size, nor morphology of particles can be controlled, as can be seen from TEM images (Fig. 2). Although sample is highly crystalline and crystal planes are clearly visible, sizes of particles are ranging from 2 to 20 nm while morphology varies from spherical particles to faceted flakes (Fig. 2b, c and d).

Our next step was to go to extreme, and to use only oleic acid, while in order to push reaction towards formation of CIS, molarity of Cd ions was decreased to 2/3 of stoichiometric value (sample C2). Diffractogram of this sample is presented in Fig. 3 (and Fig. S2 in ESI).

Clearly, the major part of material is in cubic crystalline form CIS (JCPDS card No. 27-0060), but there are still few low – intensity peaks that most probably originate from hexagonal CdS. Existence of well-defined sharp peaks that are broad at the low intensity and form so called “hills”, at lower degrees region, indicated simultaneous presence of well – crystallized crystal domains together with crystal domains of just few nanometers. Using X-ray Line Profile Fitting Program (XFIT)<sup>22</sup> we calculated that coherent domain sizes of larger fraction/particles in sample is about 29 nm. Co-existence of two types of materials in sample C2 is confirmed with TEM images (Fig. 4a). SAED confirmed existence of CdS and CIS in sample (Fig. 4d). According to XRD pattern larger particles originated from CIS (Fig. 4b), while particles of about 4 nm are

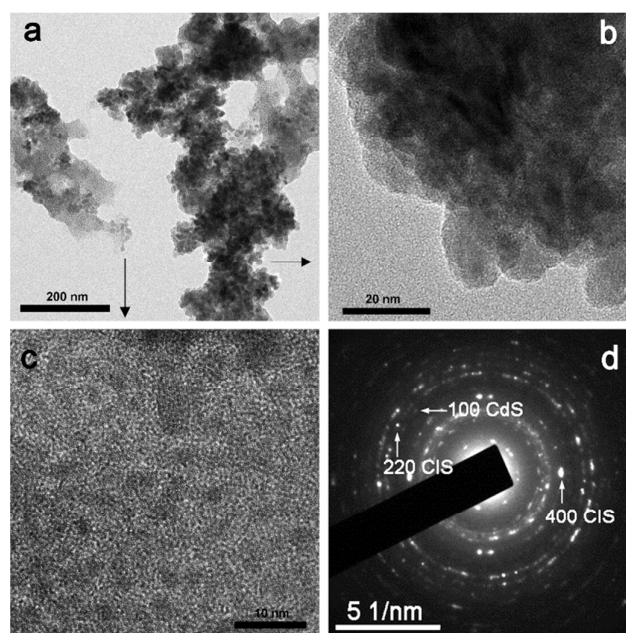


**Fig. 4** TEM images (a, b, c) of sample C2, synthesized in oleic acid, d) SAED pattern

CdS (Fig. 4c). Interestingly, there is certain uniformity in particle sizes in both groups (indicated by the arrows in Fig. 4a).

Diffractograms and TEM images of both samples gave us a hint/tip about growth mechanism of CIS. Since in both samples there is CdS, it seems that initially CdS nanoparticles are formed, while later through cation exchange process Cd ions are partially replaced with In ions, with formation of CIS as final product. This means that reaction between ions needs to be accelerated. One of the ways how this can be achieved is to speed up degradation of metal-oleic acid complex by addition of oleylamine, which, as organic base, enables faster decomposition of these complexes.<sup>23</sup> Bearing in mind that OLAM is also reducing agent and may serve as weak capping agent, we have kept volume of oleic acid higher than that of OLAM, so final volume ratio was OA:OLAM=4:1. In order to track influence of OLAM addition, reaction time varied from 15 min to 1h. XRD patterns of these samples are presented in Fig. 5 (and Fig. S3 in ESI).

After 15 min, peak at about 20.8 ° dominates over diffractogram, which, we believe, originates from metal-oleic acid complexes. The rest of diffractogram (from 22-60 deg) indicates only a presence of amorphous forms, with the exception of sharp peak at 28.6°, which can be attributed to (222) plane of cubic CIS. After 30 min, there are still some residues from metal-oleate, but majority of sample is CIS (due to peak intensity ratio, as can be seen in Fig. 5). XRD of this sample underlined two major points:

1. Even if OLAM is added, decomposition of metal-oleate and subsequent nucleation is process that controls overall kinetics of CIS synthesis

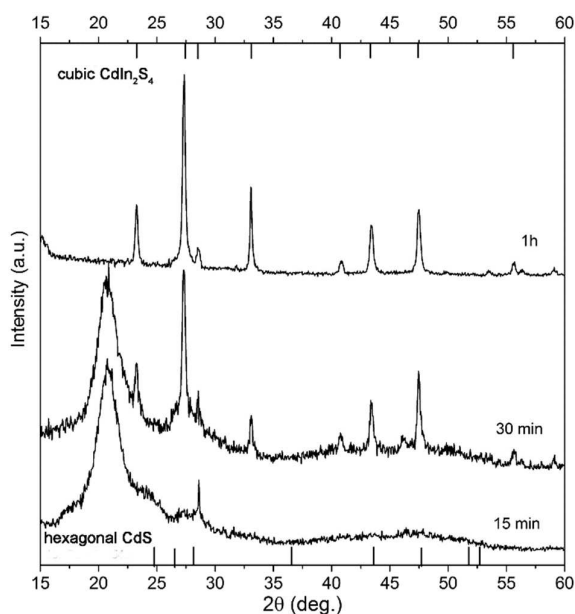


**Fig. 5** XRD pattern of sample synthesized with OA/OLAM ratio 4/1, taken after 15, 30 min and 1h (C3).

2. XRD indicates presence of both, metal-oleate complexes and CIS, which means that nucleation and growth are two simultaneous processes in these reaction conditions.

Finally, after 1h we presumed that reaction is over, and peaks from XRD match to pure cubic CIS, with no detectable presence of binary sulfides or metals. By addition of OLAM, comparing to synthesis in pure OA, reaction time decreased from 4h to 1h, and also pure CIS phase is synthesized. By applying XFIT on each diffraction peak we have calculated coherent domain sizes for C3 (Table 2). Calculated crystal domain sizes are very similar for all diffractions; majority of the domains are in the range from 22 to 28 nm, except for (400) crystal diffraction plane, for which calculated value is about 40 nm.

Diffraction plane	2θ (deg.) exp.	2θ (deg.) (JCPDS27-060)	Crystal domain (nm) (calc.)
220	23.26	23.18	28.1
311	27.33	27.24	26.7
222	28.56	28.48	28.0
<b>400</b>	<b>33.08</b>	<b>33.0</b>	<b>39.6</b>
422	40.83	40.73	22.2
511	43.42	43.31	24.6
440	47.48	47.40	26.2

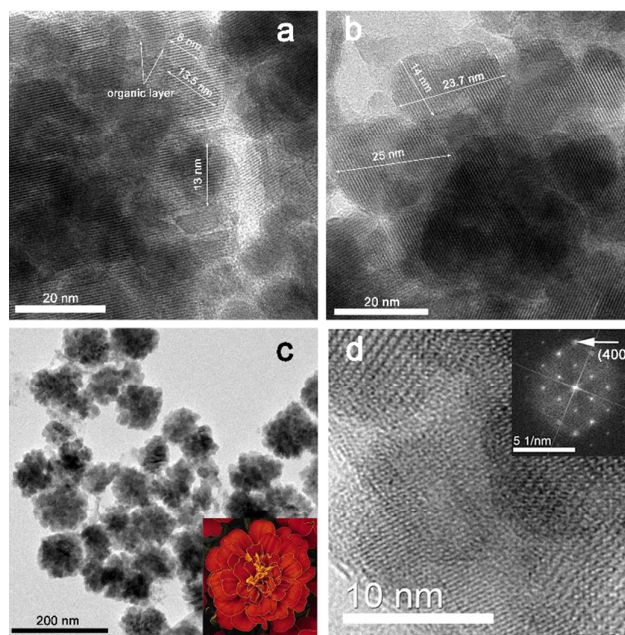


**Fig. 6** Representative TEM (a,b,c,d) images of sample C3, synthesized in OA/OLAM and FFT analysis (inset in d).

This difference could be indication that crystal domains preferentially grow along (400) direction.

TEM images (Fig. 6) revealed that OA/OLAM combination provides convenient environment for formation of complex hierarchical morphologies. From Fig. 6a it is visible presence of small subunits with diameters ranging from 8 to 14 nm, interspaced by organic layer at the surface (indicated by the arrows). Existence of organic capping agents on their surface facilitates rotation of these subunits, so they can share common crystal plane, and through oriented attachment process form bigger structures known as mesocrystals.<sup>24-26</sup> Namely, classical crystallization process can be represented as: ions/atoms/molecules → clusters → nanocrystals → single crystal. On the contrary, non-classical crystallization takes nanocrystal as primary building block. In the next step, nanocrystals orientate in such a manner to share common crystal plane and attach to each other or merge, forming bigger structure known as mesocrystal.<sup>25</sup> If primary nanocrystals have organic molecules attached on their surface, this way of growth through fusion of primary subunits will lead to inclusion of organic molecules in mesocrystal structure and formation of defects. This mode of material growth can lead to the differences in crystal sizes calculated from XRD data and seen from TEM images. Namely, nanocrystalline subunits in mesocrystal are oriented almost perfectly, so corresponding diffraction pattern will be very similar to that of single crystal.<sup>24</sup> However, building subunits can be interspaced by organic layer, so existence of these defects make them observable by TEM. This is also a reason why calculated values from XRD data are higher. Anyhow, from Fig. 6b, it is clear that mesocrystals have diameters ranging from 20 to 30 nm, which is in good agreement with calculated crystal domain sizes.

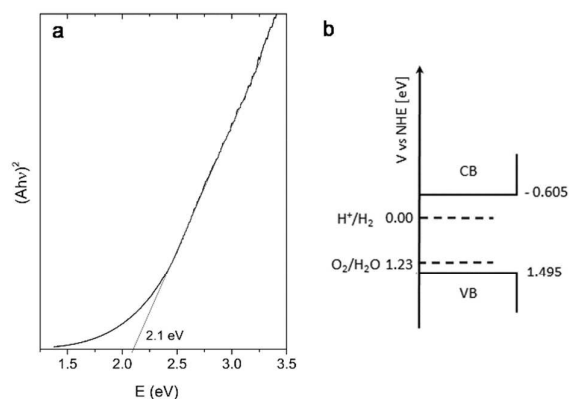


**Fig 7.** a) Tauc plot of sample C3, b) positions of calculated band edges versus NHE

Obtained mesocrystals are self-organized in marigold-structures (Figure 6c) and highly crystalline. The well-ordered crystalline planes are clearly seen all over marigold structure, although individual smaller nanoparticles, subunits, can also be seen. Similar marigold superstructures can be found in literature,<sup>2,4,5,11,12</sup> but, as far as we know, their growth through mesocrystal arrangement is not reported till now. Fig. 6d represents one fragment of marigold-like structures and matching FFT analysis. Spot indicated by arrow corresponds to (400) planes.

In order to evaluate optical properties of C3, UV-Vis absorption spectrum was recorded, and then presented as Tauc plot (Fig. 7a). By extrapolation of linear region of this plot we have estimated that band-gap energy of this sample is far in the visible part of the spectra and has a value of  $\sim 2.1$  eV. Besides value of band-gap, very important parameters that determine if some material is suitable for water splitting, and photocatalytic applications at all, are relative potentials at which semiconductor's conduction and valence band edges are suited. For successful application, it is necessary that edge potential of conduction band (CB) is suited above  $H^+/H_2$  potential, while valence band (VB) edge potential should be below oxygen evolution level. The easiest way to calculate these values is by using empirical equation related to electronegativity<sup>27</sup>

$$E_{CB,VB} = E_0 + (\chi_{cd} + \chi_{in}^2 + \chi_s^4)^{1/7} \pm 1/2 E_g$$

where  $\chi$  is absolute electronegativity,  $E_g$  is estimated band-gap energy of semiconductor, while  $E_0$  represents difference between normal hydrogen electrode (NHE) and the vacuum, and has the value of -4.5 eV.

According to this equation, bottom of conduction band of C3 is situated at -0.605 eV, while top of the valence band is at 1.495 eV. These calculated potentials are schematically depicted at Fig. 7b. As can be seen calculated positions of band edges are properly positioned versus  $H^+/H_2$  and  $O_2/H_2O$  potentials. According to this, obtained sample could be considered as appropriate material for water splitting.

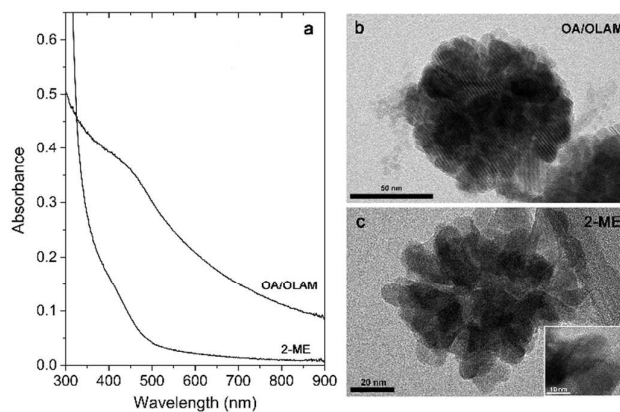


**Fig. 8** a) Adjacent UV/Vis spectra of sample C3 capped with OA/OLAM dispersed in toluene and 2-ME dispersed in water; b) TEM image of "marigold" capped with OA/OLAM; c) TEM image of "marigold" capped with 2-ME. Inset: Enlarged fragment of "marigold" capped with 2-ME.

However, for the most applications one of the requests is possibility of working in the aqueous media. As synthesized particles are capped with combination of organic OA/OLAM molecules, it was necessary to exchange these surface ligands with some hydrophilic molecule. For this purpose we have chosen 2-mercaptoethanol ( $HS-CH_2-CH_2-OH$ , 2-ME) since it has mercapto (-SH) group, which enables easy bonding to cations on CIS particles surface, and hydrophilic hydroxyl (-OH) group. Adjacent absorption spectra of sample C3 capped with OA/OLAM and capped with 2-ME are presented in Fig. 8a. Upon surface ligand exchange, main optical characteristics were preserved, but it is also interesting to notice that for 2-ME capped sample in long wavelength region there is less light scattering; sign that particles/agglomerates are better dispersed. Actually, from TEM images (Figs. 8b and c, Figs. S5 and S6 in ESI) it is clear that while crystallinity (inset) and size of the mesocrystalline agglomerates are preserved, structure is less compacted. Such dispersions stayed stable for few months, without any precipitation, even if they were kept at room temperature, not protected from light, which is good recommendation for this way of organic/water transfer. Here, it should be stressed that mesocrystal could be considered as "nanoparticles that are glued together by inorganic or organic linker".<sup>26</sup> If a nature of the "glue" is changed, it could be expected that properties of mesocrystal will change. Properties of mesocrystal are usually inherited from building nanoparticles, but if fusion between these primary building blocks is achieved, new-formed mesocrystal could have some new and enhanced characteristics (specific surface area, porosity, photocatalytic activity, etc.). Anyhow, whether mesocrystals are considered for application in photocatalysis, solar energy conversion or optoelectronics, they need to be well characterized, and compared with their nanocrystalline and single-crystal counterparts.<sup>24-26</sup>

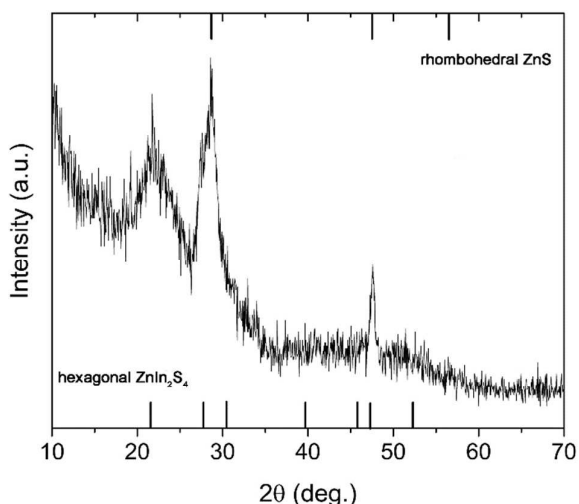


Fig. 9 XRD pattern of sample Z1 synthesized in OA/OLAM=2/1

### ZnIn<sub>2</sub>S<sub>4</sub>

In order to check if it is possible to use the same general method of synthesis for the other three-component semiconductors, we have chosen to synthesize ZIS, another semiconductor from II-III<sub>2</sub>-VI<sub>4</sub> family. As Bae et al.<sup>28</sup> suggested, Cd<sup>2+</sup> has weaker binding energy with oleic acid than Zn<sup>2+</sup>, hence the same principles of OLAM usage was tried for synthesis of ZnIn<sub>2</sub>S<sub>4</sub>. Considering this difference between strengths of metal – oleic bonds, volume of OLAM was increased, so final ratio was OA/OLAM=2/1. Reaction was stopped after 30 min, in order to see early stages of nucleation and growth, and to characterize the system in intermediate state. XRD pattern of this sample (Z1) (Fig. 9 and Fig. S7 in ESI) revealed a presence of both hexagonal ZIS (JCPDS No.065-2023) and rhombohedral ZnS (JCPDS No. 089-2181). Peaks of these two phases are at very similar 2θ values, so it was not possible to calculate crystallite sizes. The only feature that unmistakably distinguishes ZIS from ZnS is peak at 21.6°, which corresponds to diffraction from (006) crystal plane. Again, existence of both, binary and ternary sulfide lead us to conclusion that ZIS grows through Zn<sup>2+</sup>/In<sup>3+</sup> cation exchange process.

Morphology of Z1 was examined by TEM (Fig. 10). Images revealed presence of small round particles, with diameters of about 3 nm (Figs. 10a and b), but also thin flakes with diameters of about 25 nm (Fig. 10a). Hexagonal ZnIn<sub>2</sub>S<sub>4</sub> has lamellar crystal structure<sup>13,29</sup> so formation of such layered structures or flakes is not unexpected. In their article from 2006, Gou et al.<sup>6</sup> have shown that reaction temperature and time are main factors that have influence of whether these layers will fold into tubes or not. In their synthesis, for temperatures higher than 180°, lamellar structures start to fold at the edges and if sample was kept at elevated temperature for the sufficient time, resulting morphology can be tubular.

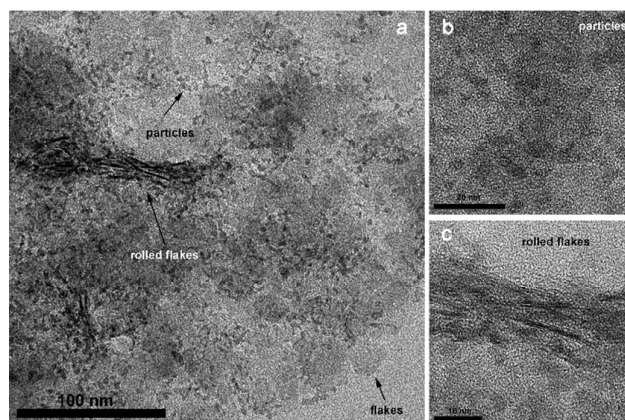


Fig. 10 TEM (a,b,c) images of sample Z1 synthesized in OA/OLAM=2/1

Our samples also showed the beginning of tube formation (Figs. 10a and c). Length of tubular structures matches well with flakes diameter. However, we believe that reaction time of 30 min was not sufficient for completion of folding and formation of tubular structure. The possible explanation can be that ZnS nucleation/ Zn<sup>2+</sup>/In<sup>3+</sup> cation exchange/flakes rolling are simultaneous processes. Anyhow, additional detailed experiments must be conducted in order to be sure that our synthetic procedure can finely lead to tubular ZnIn<sub>2</sub>S<sub>4</sub>.

### Conclusions

Hot-injection method for synthesis of CIS is presented. Influence of different organic reaction media on CIS formation is followed and explained, and it was found that for given experimental conditions pure CIS can be synthesized only in combination of OA and OLAM. It is proposed that CIS grows from binary CdS through Cd/In cation exchange process. Synthesized particles with about 25 nm in diameter are self-organized in marigold-like mesocrystal structures. By using empirical equation we have calculated positions of conduction (-0.605 V) and valence band (1.495 V) edges of synthesized CIS. According to these calculated values, synthesized material could be considered as appropriate material for water splitting.

Furthermore, we have proposed easy way to transfer CIS from organic phase to water media, by using 2-ME. Upon transfer, all main characteristics of material are preserved, but also better stability of obtained dispersions is achieved. Mainly, mesocrystalline structure of marigold agglomerates is preserved making applications, which demand water as a medium, of these materials feasible.

Additionally, initial experiments in synthesis of ZIS by using OA/OLAM combination are presented. Mixed binary/ternary sulfides are obtained. Ternary sulfides grow in forms of flakes, that, probably, during time, start to roll, forming tubes. Future work will be directed towards synthesis of pure ZIS, as well as clarifying its nucleation, growth and tube formation mechanism.

## Acknowledgements

Financial support for this study was granted by the Ministry of Education and Science of the Republic of Serbia (Projects: III45020 and OI172056) and COST actions CM1101 and MP1106.

## Notes and references

- 1 W. Shangguan, A. Yoshida, *J. Phys. Chem. B.* 2002, **106**, 12227.
- 2 B. B. Kale, J.-O. Baeg, S.M. Lee, *Adv. Funct. Mater.* 2006, **16**, 1349.
- 3 L. Fan, R. Guo, *R. J. Phys. Chem. C* 2008, **112**, 17000.
- 4 W. Jiang, X. Yin, F. Xin, Y. Bi, Y. Liu, X. Li, *Appl. Surf. Sci.* 2014, **288**, 138.
- 5 A. Bhirud, N. Chaudhari, L. Nikam, R. Sonawane, K. Patil, J.-O. Baeg, B. Kale, *Int. J. Hydrogen Energ.* 2011, **36**, 11628.
- 6 X. Gou, F. Cheng, Y. Shi, L. Zhang, S. Peng, J. Chen, P. J. Shen, *Am. Chem. Soc.* 2006, **128**, 7222.
- 7 J. Zhou, G. Tian, Y. Chen, X. Meng, Y. Shi, X. Cao, K. Pan, H. Fu, *Chem. Commun.* 2013, **49**, 2237.
- 8 S.N. Baek, T.S. Jeong, C.J. Youn, K.J. Hong, J.S. Park, D.C. Shin, Y.T. Yoo, *J. Cryst. Growth* 2004, **262**, 259.
- 9 L. Ye, J. Fu, Z. Xu, R. Yuan, Z. Li, *ACS Appl. Mater. Inter.* 2014, **6**, 3483.
- 10 X. Hu, J.C. Yu, J. Gong, Q. Li, *Cryst. Growth Des.* 2007, **7(12)**, 2444.
- 11 S.K. Apte, S.N. Garaje, R.D. Bolade, J.D. Ambekar, M.V. Kulkarni, S.D. Naik, S.W. Gosavi, J.-O. Baeg, B. B. Kale, *J. Mater. Chem.* 2010, **20**, 6095.
- 12 W. Wang, T. W. Ng, W. K Ho, J. Huang, S. Liang, T. An, G. Li, J.C. Yu, P.K. Wong, *Appl. Catal. B-Environ.* 2013, **129**, 482.
- 13 L. Shang, C. Zhou, T. Bian, H. Yu, L.-Z. Wu, C.-H. Tung, T. Zhang, *J. Mater. Chem. A* 2013, **1**, 4552.
- 14 S. Peng, L. Li, Y. Wu, L. Ji, L. Tian, M. Srinivasan, S. Ramakrishna, Q. Yan, S.G. Mhaisalkar, *CrystEngComm* 2013, **15**, 1922.
- 15 S. Peng, S. G. Mhaisalkara, S. Ramakrishna, *Mater. Lett.* 2012, **79**, 216.
- 16 J. Feng, H. Zhu, X. Wang, X. Yang, *Chem. Commun.* 2012, **48**, 5452.
- 17 C. B. Murray, D. J. Norris, M. G. Bawendi, *J. Am. Chem. Soc.* 1993, **115**, 8706.
- 18 N. D. Abazović, M. I. Čomor, M.N. Mitrić, E. Piscopiello, T. Radetić, I.A. Janković, J.M. Nedeljković, *J. Nanopart. Res.* 2012, **14**, 810.
- 19 M.V. Beloš, N.D. Abazović, J. Kuljanin Jakovljević, I. Janković, S.P. Ahrenkiel, M. Mitrić, M.I. Čomor, *J. Nanopart. Res.* 2013, **15**, 2148.
- 20 W. W. Yu, X. Peng, *Angew. Chem., Int. Ed.* 2002, **41**, 2368.
- 21 D. Battaglia, X. Peng, *Nano Lett.* 2002, **2**, 1027.
- 22 R.W. Cheary, A.A. Coelho, *J. Appl. Cryst.* 1992, **25**, 109.
- 23 N. Bao, X. Qiu, Y.-H. A. Wang, Z. Zhou, X. Lu, C.A. Grimes, A. Gupta, *Chem. Commun.* 2011, **47**, 9441.
- 24 H. Cölfen, M. Antonietti, *Angew. Chem. Int. Ed.* 2005, **44**, 5576.
- 25 Y. Liu, Y. Zhang, J. Wang, *CrystEngComm*, 2014, **16**, 5948.
- 26 L. Zhou, P. O'Brien, *J. Phys. Chem. Lett.* 2012, **3**, 620.
- 27 Y. Xu, M.A.A. Schoonen, *Am. Mineral.* 2000, **85**, 543.
- 27 W.K. Bae, M.K. Nam, K. Char, S. Lee, *Chem. Mater.* 2008, **20**, 5307.
- 28 L. Shi, P. Yin, Y. Dai, *Langmuir* 2013, **29**, 12818.

CdIn<sub>2</sub>S<sub>4</sub> merigold-like mesocrystals formation in oleic acid/oleylamine media.